Article ID: 1003－6326(2005)04－0855－08

Preparation and H^+ response mechanism of W/WO_3 pH electrode by sol-gel method①

CHEN Dong-chu(陈东初)[1], FU Chao-yang(付朝阳)[2],
ZHEN Jia-sheng(郑家燊)[2], WANG Zhe(王 哲)[2]
(1. School of Science, Foshan University, Foshan 528000, China;
2. Department of Chemistry, Huazhong University of Science and Technology, Wuhan 430074, China)

Abstract: A method of sol-gel for preparing a W/WO_3 pH electrode was presented. H^+ response characteristics, such as response range, response sensitivity, response time were investigated. The effect of heat-treatment on response linear relation was discussed. The influences of interfered ions and solution temperatures were also taken into consideration. Many kinds of determination technology, such as TG, DSC, IR, SEM, AFM, XPS, XRD were used to characterize the film. The results show that the film appears in crack dried-mud, and the film is composed of WO_3, $WO_3 \cdot H_2O$ or $WO_3 \cdot 0.33H_2O$; the hydrate water decreases with the increase of the heat-treatment temperature; the W^{+6} in the electrode film transfers to W^{+5} in the course of H^+ response; the H^+ response course is controlled by the H^+ diffusion from the solution to the WO_3 crystalline, which is indicated in the EIS spectra; the best heat-treatment temperature is 200 ℃, and at this temperature, the electrode has an H^+ response sensitivity of 52 mV/pH.

Key words: sol-gel; W/WO_3; pH electrode; film composition; H^+ respouse mechanism
CLC number: TB34 **Document code:** A

1 INTRODUCTION

Acidity is one of the most important parameters in aqueous samples. Although the glass electrode is by far the most commonly used pH sensor, limitations of the glass electrode, such as acid and alkaline error, high impedance, high temperature instability and mechanical fragility restrict its further application to pH determination in the wider range[1]. Therefore, the research interest has been directed toward the development of alternatives to conventional glass electrode.

Many metal oxides not only exhibit a good response to H^+, but also are inherently stable in aggressive environments at high temperature and high pressure or in F^- containing solutions. In addition, the good mechanical strength makes it easy to miniaturize. Various metal oxides have been suggested to be used as pH sensing electrodes, such as MnO_2, PbO_2, WO_3, Co_3O_4, TiO_2, PtO_2, RuO_2, RhO_2, OsO_2 and IrO_2[2-6].

Sol-gel technology is believed as a convenient method to control the film composition and the micro-morphology with inexpensive coating equipment, and it is attempted to take place of the traditional film formation method in many fields, such as in the fabrication of protective coatings, YSZ membrane, reflective optical coating, storage systems, self-assemble monolayers, and gas sensitivity thin film[7-10]. WO_3 is commonly investigated as the electrochromic material, and the sol-gel process is accepted as a new method, which attracts much interest in these years. It switches reversibly from white to blue upon electrochemical redox reaction with the injection and extraction of electrons and cations (mainly H^+ and Li^+) as follows: $xM^+ + WO_3 + xe^- \rightarrow M_xWO_3$ (M: H^+, Li^+), which could take place even in the situation of absence of any applied voltage[11].

According to many reports, the sol-gel technology of WO_3 has shown perspects to the preparation of NO_x sensor[12]. As far as it is known, the WO_3 oxide could be prepared for the H^+ selective film with three methods, i. e. chemical oxidization, cyclic voltammetry electro-chemical oxidization and sputtering[13-15]. In this paper, a method is attempted to prepare a H^+ selective film based on sol-gel technology, which shows the potential application to pH electrode for its lower cost, compared with the reported pH electrode based on the expensive material of Ir, Ru, Rh, etc.

The tungsten trioxide could combine with

① **Foundation item:** Project supported by the Research Foundation of Foshan University
Received date: 2004－09－23; **Accepted date:** 2004－12－21
Correspondence: CHEN Dong-chu, PhD; Tel: +86-757-82988684; E-mail: cdcever@tom.com

water molecules to form crystalline $WO_3 \cdot nH_2O$ (n= 2, 1 or 1/3), or amorphous metatungstic acids and isopoly-tungstic acids[16]. The H^+ response characteristic of the W/WO_3 electrode was related to the composition and morphology of the hydrous tungsten oxide, therefore various determination methods such as TG, DSC, IR, SEM, AFM, XRD, XPS were used to characterize the film. As the H^+ sensitive material, the W/WO_3 film worked through a H^+ involved reaction. The H^+ response was not only related to the thermodynamic equilibrium but also to the dynamics course. The EIS experiment was carried out to investigate the control step in the dynamics course of the H^+ response.

2 EXPERIMENTAL

2.1 Preparation of WO_3 sol

The sol was prepared with an ion-exchange method, which could be found in many references[16], and the process was as follows: a commercial cation-exchange resin (001 × 7, Nankai chemical Co.) was immersed in an acid solution (10% HCl) for 1 h to convert it from Na^+ to H^+ type. After being washed with distilled water for several times, the resin was packed uniformly in a glass column and washed again with distilled water repeatedly until the pH of the effluent was close to 7. The ion-exchange capacity (content of protons) of the resin was about 1.8×10^{-3} mol Na^+ / 1 mL resin, which was obtained from the product manual. The solution of 0.4 mol/L Na_2WO_4 was let to flow down through the glass column at a fixed rate, and the effluent was collected into a beaker. Such chelants as H_2O_2 and C_2H_5OH were added to WO_3 sol with appropriate content for the purpose of avoiding the formation of WO_3 gel.

2.2 Fabrication of W/WO_3 pH electrode

Tungsten oxide film was coated on the surface of tungsten wire(d0.5 mm) by dipping the wires into the tungsten sol, and then a heat treatments at 100 ℃, 200 ℃, 300 ℃, 400 ℃ respectively were carried out in oven. A thick film was formed when repeating the above process, and the thickness of the oxide film was controlled by the dipping time. The composition and molecular structure of the oxide were dependent of the thermal treatment temperature.

To prepare the pH electrode, a small section at one end of the coated wire was scraped off, and Cu wire with a length of 10 cm was spot-welded on the exposed base metal to form an ohmic contact. This junction as well as Cu wire was sealed with heat-shrink silicone adhesive or epoxy resin so that only the tungsten oxide surface was exposed.

2.3 pH response measurement

Open-circuit potential of the W/WO_3 electrode was measured as a function of pH value of the test solution against a single junction saturated Calomel reference electrode by using a potentiostat (the input resistance > 10^{12} Ω). Before measurement, W/WO_3 electrode was stored in distilled water. All the potentiometric measurements were performed in an air-saturated buffer solution at room temperature. The buffer solution consisted of 0.01 mol/L $CH_3COOH/HBO_3/H_3PO_4$ and 0.1 mol/L KCl[17]. The pH of the buffer solution was varied by dropwise addition of 0.1 mol/L KOH or 0.1 mol/L HCl. A previously calibrated glass electrode and a digital pH meter were used to monitor the solution pH .

2.4 Microscope analysis

TG and DSC were used to analyze the change of the sol in the course of heat-treatment, and IR was also used to observe the change of the group in tungsten acid. XPS was used to determine the elements composition and the valence of W. The crystalline structures of the obtained hydrous tungsten oxides were determined by XRD. The morphology of the oxide film was observed by SEM and AFM.

2.5 EIS measurements

EIS was used to investigate the control step in the dynamics course of the H^+ response. Impedance measurements were carried out using electrochemical workstation (Zahner, German) and a managing software (Ime6). 0.01 mol/L $CH_3COOH/HBO_3/H_3PO_4$/0.1 mol/L KCl buffer was adopted as the working solution. At each fixed potential, frequencies were scanned between 5 mHz and 100 kHz. The experimental data were fitted to an equivalent circuit using Zview software.

3 RESULTS AND DISCUSSION

3.1 Response sensitivity and response time

Fig. 1 shows the relationship between open-circuit potential and pH value for the electrode heat-treated at 200 ℃. It is found that the H^+ linear response range is pH 2 – 11, with a response sensitivity of 52.6 mV/pH. The heat-treatment temperature makes some effect to the response sensitivity, therefore the electrodes prepared at different thermal treatment temperatures differ in the response characteristics. It is observed that W/WO_3 electrodes prepared at 300 ℃ and 400 ℃ have an inferior sensitivity to the sample prepared at 200

℃ in the same pH response range (2 - 11), which are respectively 39.1 and 37.4 mV/pH. The above discovery can be explained by the theory that the response characteristic is dependent of the film morphology and composition, and the thermal treatment temperature makes a considerable effect on the film characteristic.

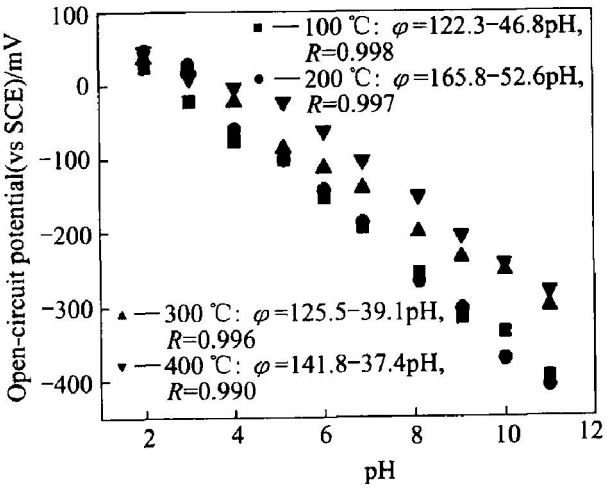

Fig. 1 Response relationship between open-circuit potential and pH for electrodes treated at different temperatures

For the convenient pH determination, the quick response of the pH electrode was needed. A computer with a specific software was used to record the open-circuit potential response. Here, $t_{95\%}$ is defined as the response time, which is 95% of the time that the electrode spends from trigger of potential response to arrival of potential steady state[18]. The response time is less than 1 min in the buffer solution of pH 2 - 11. Figs. 2(a) and 2(b) show the record of the response of the open-circuit potential of W/WO_3 electrode in pH 4.01 and pH 9.06 buffer solution respectively. The response time of the electrode is affected by the pH and temperature of the solution. Response to low pH value solution is more quick than to alkaline solution, and elevated temperature would also shorten the response time. The observed phenomena maybe result from the truth that the dynamic response of the electrode is related to the H^+ diffusion.

3.2 Anti-interference and temperature effect

The pH electrode response behavior should be stable in the solutions containing various ions, so the ion selectivity of the W/WO_3 pH electrode against major interfering ions was studied with a mixed-ion interfered method, as listed in Table 1. Table 1 lists the results of ion selectivity coefficients as $\log K_{M,H}$. The data prove that the W/WO_3 electrode is well selective to many ions except

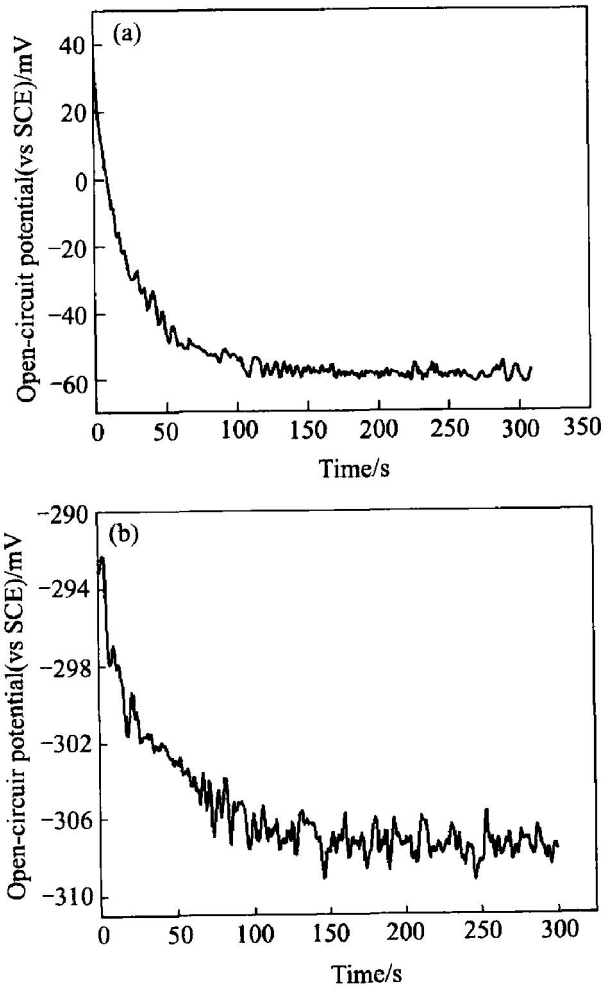

Fig. 2 Potential response of W/WO_3 electrode in buffer solution
(a) —pH = 4.01; (b) —pH = 9.06

the oxidative NO_3^-. Addition of 0.1 mol/L NO_3^- has some effect on the H^+ response relationship. Fig. 3 shows the electrode response potential in the buffer containing 0.1 mol/L NO_3^-. It shows remarkable change on the intercept and slope of the response relationship. It has been reported that the coated Nafion film will improve the H^+ selectivity of the pH electrode and the resistance to interference of negative ions[18]. It is found that the H^+ response is very slow here in the case that the electrode is coated with one or two layers of Nafion films.

Table 1 Ion selective coefficients of W/WO_3 electrode

Interfered ions	$\log K_{M,H}$	Interfered ions	$\log K_{M,H}$
Na^+	< - 10	F^-	< - 6
K^+	< - 10	I^-	< - 4
Ca^{2+}	< - 10	NO_3^-	< - 4

The electrode remains good linear response relationship in solutions at different temperatures, but its response sensitivity changes. The response

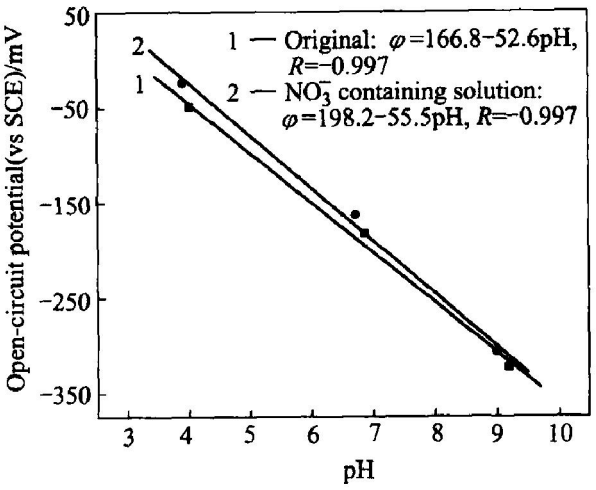

Fig. 3 Oxidate NO_3^- inference to φ—pH response relationship of W/WO_3 electrode

sensitivity is 52.4 mV/pH, 54.9 mV/pH, 57.6 mV/pH, 59.5 mV/pH respectively, corresponding to the temperature of 25 ℃, 35 ℃, 45 ℃, 55 ℃, which corresponds well with Nernst slope of the H^+ involved reaction of the electrode response. As a temperature effect, the elevated temperature would also improve the response speed.

3.3 Characte3rization of film composition and morphology

The TG and DSC curves of the gel are shown in Fig. 4. Three mass loss stages in TG curve are observed at 20 - 100 ℃, 100 - 250 ℃, > 250 ℃. The remarkable decrease in TG curve between 20 and 250 ℃ results from the loss of water, which is mainly gas evolution of absorbing water and the dehydration of hydrate water as well as the condensation of W—OH. There is little mass loss above 250 ℃. Corresponding to these mass losses, three endothermic peaks are observed. The first endothermic peaks (100 ℃), the second endorthermic peak(120 ℃), and the last endothermic peaks (250 ℃) are respectively attributed to the loss of absorbed water, the condensation of peroxotungstic acid, the loss of hydrate water and the condensation of W—OH. No crystalline transition peaks are seen in the DSC spectroscopy. From the above analysis, the conclusion could be drawn that the change of the gel film in the heat treatment course below 600 ℃ is the loss of absorbing and hydrate water, as well as condensation of W—OH, without crystalline transition taking place.

Infrared spectroscopy indicates hydration and hydroxylation. The IR spectra are shown in Fig. 5. The presence of the broad band centered around 3 400 cm^{-1} (—OH stretching) and at 1 650 cm^{-1} (—OH bending) band shows the presence of the

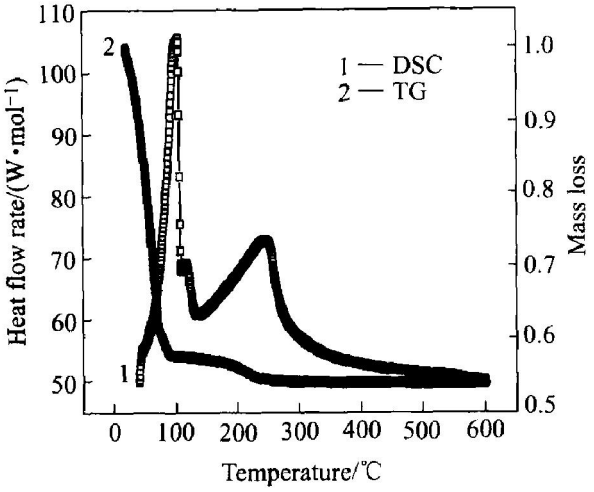

Fig. 4 TG and DSC curves of WO_3 gel

hydrate WO_3. The higher frequency band (650 cm^{-1}) belongs to the W—O—W stretching vibration, while 980 cm^{-1} is ascribed to absorption of W—O_d binding. With increasing temperature(200 ℃, 300 ℃), the W—O band appears to be more intense, while the absorption peaks at 3 400, 1 650 cm^{-1} decrease remarkably, which indicates the large loss of hydrate water. After a course of 400 ℃ heat treatment, the W—OH absorption peak at 1 400 cm^{-1} almost disappears totally.

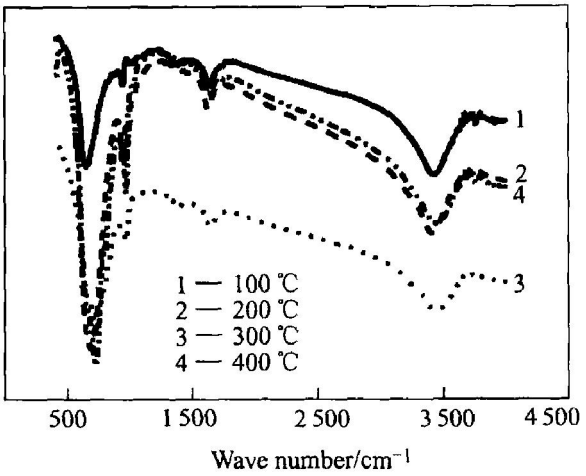

Fig. 5 IR spectra of different heat-treated WO_3 gels

XRD is able to provide detailed structure information. The oxide treated at 100 ℃ or 200 ℃ mainly shows the diffraction of WO_3 and $WO_3 \cdot H_2O$, while the intense diffractive peak of $WO_3 \cdot 0.33H_2O$ is instead of $WO_3 \cdot H_2O$ with the increase of heat-treated temperature up to 300 ℃ or 400 ℃. This result is correspondent well with the analysis of TG, DSC, which shows the dehydration of the gel in the course of heat-treatment. Fig. 6 shows XRD patterns of the gel heat-treated at 200 ℃, which shows that the film is composed of WO_3 and $WO_3 \cdot H_2O$.

XPS was used to determine the element com-

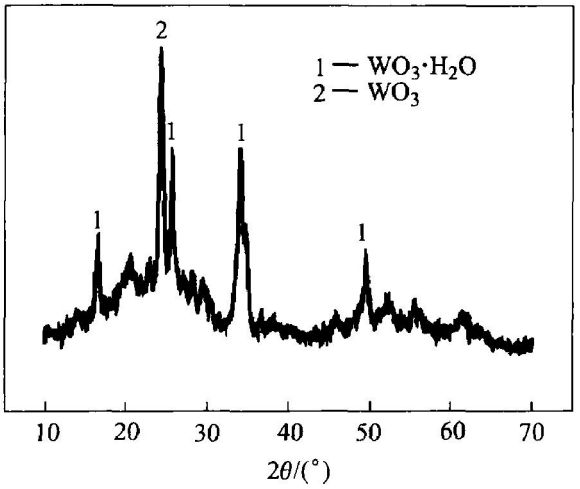

Fig. 6 XRD pattern of WO_3 processed at 200 ℃

position and the valence of W. As seen in Fig. 7, the tungsten oxide film is mainly composed of W, O, and Na^+ is exchanged completely with the cation-exchange resin. The binding energy (B. E.) of W $4f_{5/2}$ is 35. 7 eV, which corresponds well with the reported binding energy of W^{+6}, so it could be drawn that the tungsten in the oxide film exists in the form of W^{+6}. The tungsten oxide electrode is imposed by a − 50 mV negative voltage to accelerate the negative reaction in the film related to H^+ response. Fig. 8 shows XPS analysis of the W element result of the electrode being imposed by an negative voltage, which shows the overlap of the W peaks of different valence. Fitted with the reported data, i. e. W(+ 5) $4f_{5/2}$= 34. 3 eV, W(+ 5) $4f_{7/2}$= 36. 5 eV, W(+ 6) $4f_{5/2}$= 35. 7 eV, W(+ 6) $4f_{7/2}$= 37. 9 eV, as shown in Fig. 9, the XPS curve of W element could be attributed to the contribution of W^{+5} and W^{+6}. Therefore, the reaction occurring on the electrode is probably $W^{+6} + e \rightarrow W^{+5}$.

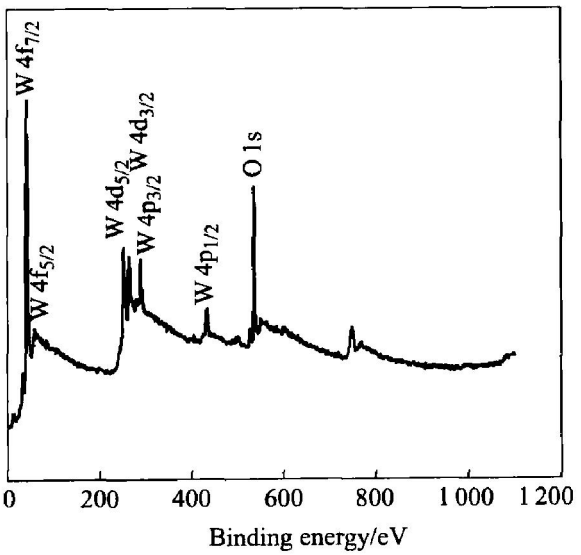

Fig. 7 XPS spectrum of electrode surface of tungsten oxide

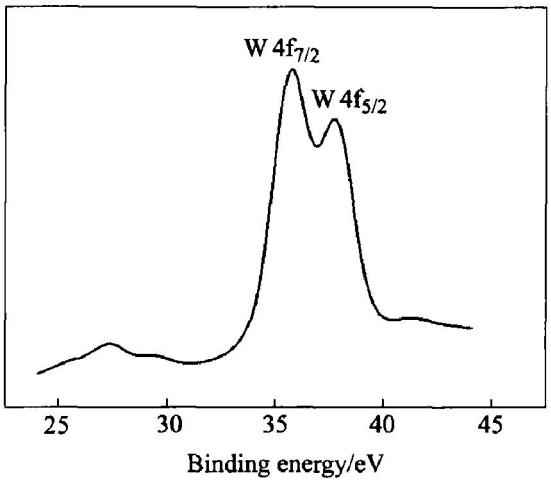

Fig. 8 XPS spectra for W element in tungsten oxide surface

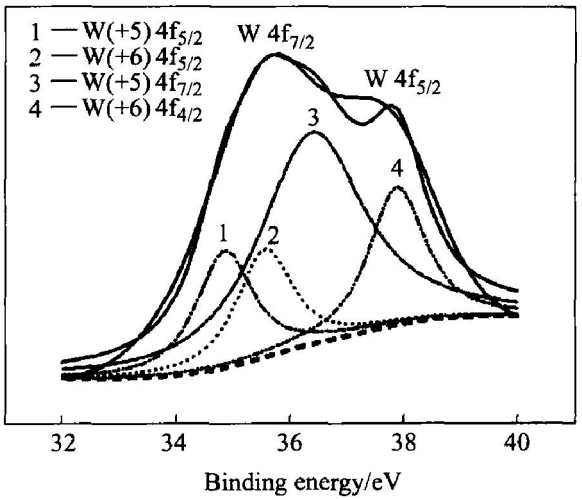

Fig. 9 XPS spectrum for W element in oxide involving H^+ response

As seen in Fig. 10 and Fig. 11, the rough WO_3 surface appears in dried crack-mud, while the crevice increases real surface area of the film.

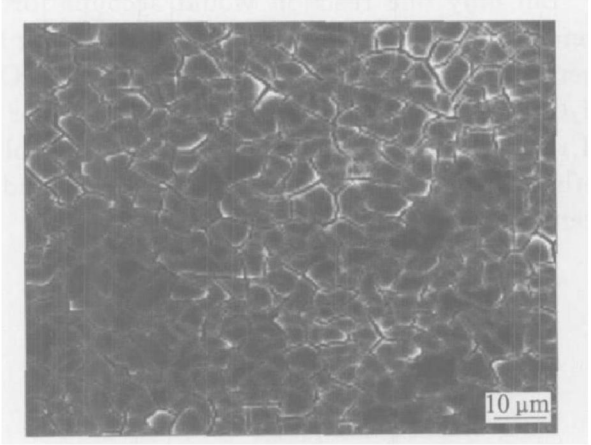

Fig. 10 SEM image of WO_3 film heat-treated at 200 ℃

The film could attach firmly to the metal base with the formation of chemical bond, i. e. W —O —

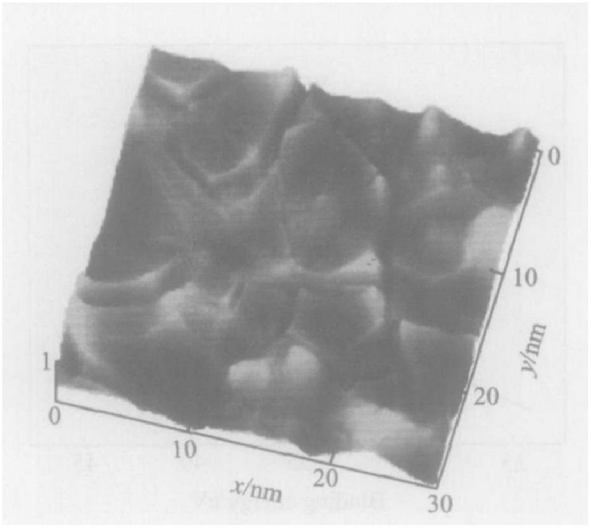

Fig. 11 AFM image of WO_3 film heat-treated at 200 ℃

W, in the heat-treatment course. The crack morphology of the WO_3 film results from the difference of thermal expansion coefficient between oxide film and base metal, as well as from the effect of capillary tension formed in gas evaporation[19]. This phenomenon is commonly observed in the sol-gel prepared film, such as TiO_2, ZrO_2 film[20]. The crevice gives a beneficial channel to H^+ transport.

3.4 Response mechanism

It can be assumed that a number of electrode reactions could result in the observed Nernst pH response, such as

$$W + xH_2O \rightarrow WO_2 + 2xH^+ + 2xe^- \quad (x = 2, 3, 12) \quad (1)$$

$$W + 4H_2O \rightarrow H_2WO_4 + 6H^+ + 6e^- \quad (2)$$

$$WO_2 + H_2O \rightarrow WO_3 + 2H^+ + 2e^- \quad (3)$$

$$WO_2 + 2H_2O \rightarrow H_2WO_4 + 2H^+ + 2e^- \text{ [21, 22]} \quad (4)$$

$$WO_3 \cdot H_2O + xH^+ + xe^- \rightarrow H_xWO_3 \cdot H_2O \text{[23]} \quad (5)$$

But only one reaction would account for the intercept on the potential axis(φ_0). Supposing that reaction (6): $WO_3 \cdot nH_2O + H^+ + e^- \rightarrow HWO_3 \cdot nH_2O$ is the reaction, which is responsible for the pH response of the W/WO_3 prepared with sol-gel method, the potential of this electrode could be given by the Nernst equation as

$$\varphi = \varphi^{\ominus} - \frac{2.303RT}{F}\log\frac{a_{HWO_3 \cdot nH_2O}}{a_{WO_3 \cdot nH_2O} \cdot a_{H^+}} \quad (7)$$

$$\varphi^{\ominus} = \varphi^{\ominus} - \frac{2.303RT}{F}\log\frac{a_{HWO_3 \cdot nH_2O}}{a_{WO_3 \cdot nH_2O}} \quad (8)$$

$$\varphi = \varphi^{\ominus} - \frac{2.303RT}{F}\log a_{H^+} \quad (9)$$

$$\varphi = \varphi^{\ominus} - 0.059\text{pH} \quad (T = 25\ ℃) \quad (10)$$

where $\varphi^{\ominus}$ depends on standard electrode potential $\varphi^{\ominus}$ and the composition of $WO_3 \cdot nH_2O$ and $HWO_3 \cdot nH_2O$.

EIS experiment is carried out to investigate the dynamic process in the course of pH response. It is known that the H^+ response is a negative reaction, and at last a balance will be arrived, as seen in reaction (6). Here the pH electrode is imposed by a negative potential for the need of dynamic study of H^+ response. Fig. 12 shows the EIS of the electrode imposed by a negative polarized potential of − 50 mV, − 100 mV and − 150 mV respectively. The results show the EIS behavior of the fractal system, with a depression of the semicircle in the higher frequency region. The depressed semicircle corresponds to a rough surface with a fractal dimension $d_f > 2$[24], and fractal behavior has been observed in earlier work on sol-gel deposited films using chronoamperometry[25]. Warburg diffusion phenomenon is shown in low frequency section of the EIS. The distorted Warburg diffusion does not display a 45° line because of the rough electrode surface[26]. The H^+ involved electrode reaction could be described to a EIS equivalent circuit, as seen in Fig. 13.

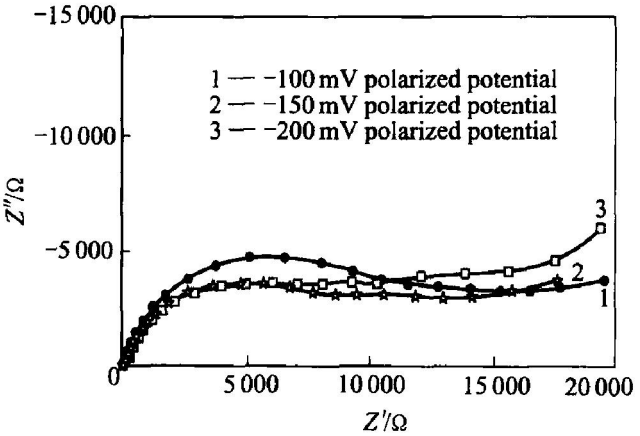

Fig. 12 EIS spectra of W/WO_3 in pH 2.0 buffer solution

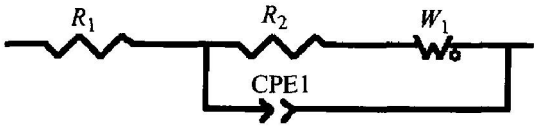

Fig. 13 EIS equivalent circuit of W/WO_3 electrode

In the course of pH response, it could be concluded that the reaction is controlled by the diffusion of H^+ from the solution into the tungsten oxide crystal. A degree content of binding water in the oxide is beneficial to the H^+ transportation[27], therefore the electrode treated at 200 ℃ has a better response sensitivity in this work.

The H^+ diffusion parameter D could be calculated with a formula as follows[28]:

$$|Z| = RT/(n^2F^2C^2\omega^{0.5}D^{0.5})$$

$$|Z| \propto \omega^{-0.5} \quad (11)$$

where $|Z|$, n, F, C, D, T, R, ω respectively represent the module of impedance, electron numbers involved in the reaction, Farady constant, solution concentration, diffusion parameter, temperature, vapor constant and angle frequency in the low frequency section of EIS experiment.

The value of D could be calculated according to Eqn. (7) and Fig. 14, which is 10^{-10} $cm^2 \cdot S$ quantitative level. Corresponding to case 1, case 2 and case 3 in Fig. 12, the values of diffusion parameter in Fig. 14 are 1.69×10^{-10}, 2.66×10^{-10}, 2.13×10^{-10} $cm^2 \cdot S$, respectively.

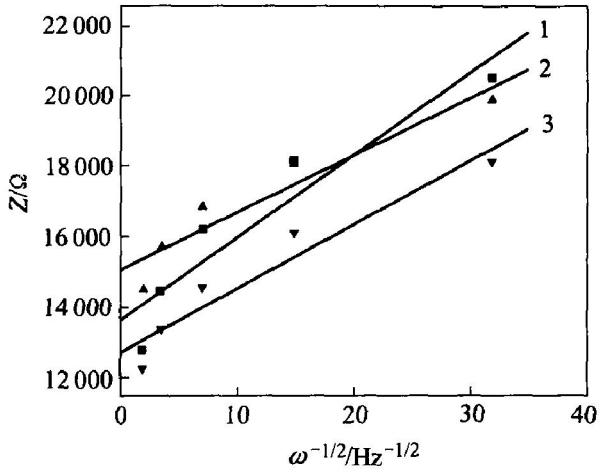

Fig. 14 Curves of $Z \propto \omega^{-0.5}$
1 —— 100 mV polarized potential;
2 —— 150 mV polarized potential;
3 —— 200 mV polarized potential

4 CONCLUSIONS

1) A method based on the sol-gel technology of WO_3 for pH electrode preparation was presented here. The pH electrode heat-treated at 100 - 400 ℃ responses in the range of pH 2 - 11, and the response sensitivity differs from each other according to the different heat-treated temperatures. The best response sensitivity of 52.6 mV/pH could be got for the electrode treated at 200 ℃.

2) The film is mainly composed of crystalline of WO_3, $WO_3 \cdot H_2O$ or $WO_3 \cdot 0.33H_2O$. The W element in the working pH eletrode is composed of W^{+5} and W^{+6}. The response reaction could be described as $WO_3 \cdot nH_2O + H^+ + e^- \rightarrow HWO_3 \cdot nH_2O$.

3) The H^+ response course is controlled by the H^+ diffusion from the solution to the WO_3 crystal. The H^+ diffusion parameter D is 10^{-10} $cm^2 \cdot S$ quantity level.

REFERENCES

[1] Shuk P, Ramanujachary K V. New metal-oxide-type pH sensors [J]. Solid State Ionics, 1996, 86 - 88(2): 1115 - 1120.

[2] Fog A, Buck R F. Electronic semiconducting oxides as pH sensors [J]. Sensors and Actuators, 1984, 5: 137 - 146.

[3] Pasztor K, Sekiguchi A, Shimo N, et al. Electrochemically-deposited RuO_2 films as pH sensors [J]. Sensors and Actuators, 1993, 13 - 14: 561 - 562.

[4] Krerder K G, Tarlor M J, Cline J P. Sputtered thin-film pH electrodes of platinum, palladiun, rutheniun, and iridiun oxides [J]. Sensors and Actuators B, 1995, 28: 167 - 172.

[5] LI Qing-wen, LUO Guo-an, SHU You-qin. Response of nano sized cobalt oxide electrodes as pH sensors [J]. Analytica Chimica Acta, 2000, 409(1 - 2): 137 - 142.

[6] Noburoshi H, Katsuhisa S. No-doped TiO_2 semiconductor pH sensor for use in high-temperature aqueous solution [J]. Journal of the Electrochemical Society, 1997, 137(8): 2517 - 2523.

[7] Lin H, Kozuka H, Yoko T. Preparation of TiO_2 films on self-assembled monolayers by sol-gel method [J]. Thin Solid Film, 1998, 315: 111 - 117.

[8] Livage J. Optical and electrical properties of vanadium oxides synthesized from alk oxides [J]. Coordination Chemistry Review, 1999, 190 - 192: 391 - 403.

[9] Baik N S, Sakai G, Shimanoe K, et al. Hydrothermal treatment of tin oxide sol solution for preparation of thin-film sensor with enhanced thermal stability and gas sensitivity [J]. Sensor and Actuators B, 2000, 65: 97 - 100.

[10] Sun Y, Sermon P A, Vong M S W. Design of reflective tantala optical coatings using sol-gel chemistry with ethanoic acid catalyst and chelator [J]. Thin Solid Films, 1996, 278: 135 - 139.

[11] Livage J, Guzman G. Aqueous precursors for electrochromic tungsten oxide hydrates [J]. Solid State Ionics, 1996, 84: 205 - 211.

[12] Lee D S, Han S D, Huh J S, et al. Nitrogen oxides-sensing characteristics of WO_3-based nanocrystalline thick film gas sensor [J]. Sensor and Actuactors B, 1999, 60: 57 - 63.

[13] Yamamoto K, SHI Guo-yue, ZHOU Tian-shu, et al. Solid-state pH ultramicrosensor based on a tungstic oxide film fabricated on a tungsten nanoelectrode and its application to the study of endothelial cells [J]. Analytica Chimica Acta, 2003, 480: 109 - 117.

[14] XIAO Feng-ying, XU Jin-rui. Preparation of multibeam-type W/WO_3 micro pH sensor [J]. Journal of Huaqiao University (Natural Science), 2001, 22(2): 158 - 160. (in Chinese)

[15] Natan M J, Mallouk T E, Mark S. Wrighton. PH-sensitive WO_3-based micro-electrochemical transistors [J]. Journal of Physics Chemistry, 1987, 91: 648 - 654.

[16] Choi Y G, Sakai G, Shimanoe K, et al. Preparation of aqueous sols of tungsten oxide dihydrate from tungstate by an ion-exchange method [J]. Sensors and Actuators B, 2002, 87: 63 - 72.

[17] SU You-qing, LI Qing-wen, LUO Guo-ang. Preparation of a nano-MnO_2 pH electrode and its use in solution containing F^- [J]. Chinese Journal of Analytical Chemistry, 2000, 28(5): 657. (in Chinese)

[18] Kinlen P J, Heider J E, Hubbard D E. A solid-state pH sensor based a nafion-coated iridium oxide indicator electrode and a polymer-based silver chloride ref-

erence electrode [J]. Sensor and Actuators B, 1994, 22: 13－25.

[19] YI Guang-hua, Michael Sayer. Sol-gel processing of complex oxide films [J]. Ceramic Bulletin, 1991, 70 (7): 1173－1179.

[20] Sugama T, Kikacka L E, Carciello N. Polytitiano-suloxane coatings derived from $Ti(OC_2H_5)_4$-modified organosilane precursors [J]. Progress in Organic Coatings, 1990, 18: 173－196.

[21] Millett P J. Tungsten/tungsten oxide pH sensing electrode for high temperature aqueous environments [J]. Journal of Electrochemistry Society, 1994, 141 (11): 3002－3005.

[22] Adhoum N, Monser L, Sadok S, et al. Flow injection potentiometric detection of trimethylamine in seafood using tungsten oxide electrode [J]. Analytica Chimica Acta, 2003, 478: 53－58.

[23] Kovach S K, Olifirenko S N, Vasko A T. On the pH sensitivity of the galvanic tingsten-water interaction product [J]. Journal of Electroanalytical Chemistry, 1999, 472: 178－181.

[24] Wang J, Bell J M, Skryabin I L. Kinetics of charge injection in sol-gel deposited WO_3 [J]. Solar Energy Materials and Solar Cells, 1999, 56: 465－475.

[25] Stromme M, Gutarra A, Niklasson G A, et al. Impedance spectroscopy on lithiated Ti oxide oxyfluoride thin films [J]. Journal of Applied Physics, 1996, 79 (7): 3749－3756.

[26] CAO Cu-nan, ZHANG Jian-qing. An Introduction to Electrochemical Impedance Spectroscopy [M]. Beijing: Science Press, 2002. 106－107. (in Chinese)

[27] ZHANG Jing-rong, CHEN Zheng, YANG Chang-sheng, et al. WO_3 electrochromic thin films prepared by sol-gel method [J]. Functional Material, 2000, 31(4): 385－387. (in Chinese)

[28] LIU Yong-hui. Electrochemical Determination Technology [M]. Beijing: Aeronautical Institute of Beijing Press, 1987. 178－180. (in Chinese)

(Edited by YANG Bing)